

Electronic Supplementary Information (ESI)

Stable hydrogen-bonded organic frameworks for selective fluorescence detection of Al³⁺ and Fe³⁺ ions

Cheng-Quan Xiao, Wen-Hai Yi, Jun-Jie Hu, Sui-Jun Liu* and He-Rui Wen*

School of Chemistry and Chemical Engineering, Jiangxi University of Science and Technology, Ganzhou 341000, Jiangxi Province, P.R. China.

E-mail: sjliu@jxust.edu.cn (S.-J. Liu), wenherui63@163.com (H.-R. Wen); Tel: +86-797-8312289, +86-797-8312204

Table S1. Hydrogen-bonding lengths (Å) and angles (°) for HOFs 1-4

D-H···A	Distance of D···A(Å)	Angle of D-H···A(°)
HOF 1		
O3–H3···N1	1.821	164.223
O1A–H1A···O5C	2.460	124.843
O7–H7···N2B	1.785	174.308
O4–H4···O1A	2.073	162.871
O6D–H9D···O2	1.835	156.867
HOF 2		
O4–H4···N1	1.784	172.250
O10–H10···O3	1.958	163.256
O6A–H6A···O9	1.925	158.795
O2–H2···O10B	2.036	161.123
O7–H7···N2C	1.833	166.666
HOF 3		
O4–H4···N2	1.706	173.196
O6–H6···N1	1.822	163.604
O3–H3···O8A	1.747	151.491
O1–H1···O5B	2.082	151.168
HOF 4		
O3–H3A···N1A	1.638	162.814
O7–H7···N3B	1.610	175.016
O1–H8···O2C	2.611	139.389
O2C–H2C···O9D	1.992	163.202
O5–H6···O6E	1.679	177.431

Symmetry codes for HOF 1: A: -x, 1-y, -z, B: x-2, 0.5-y, z-0.5, C: x, 0.5-y, z-0.5, D: 1-x, -y, 1-z. HOF 2: A 2-x, -y, 2-z, B: -x, 1-y, 1-z, C: 2+x, 0.5-y, 0.5+z. HOF 3: A: 1-x, -y, 2-z, B: 1-x, 1-y, 1-z. HOF 4: A: x+1, y, z, B: x-1, y, z, C: x+0.5, 0.5+y, z-0.5, D: -x, 1-y, 1-z, E: -x, -y, -z.

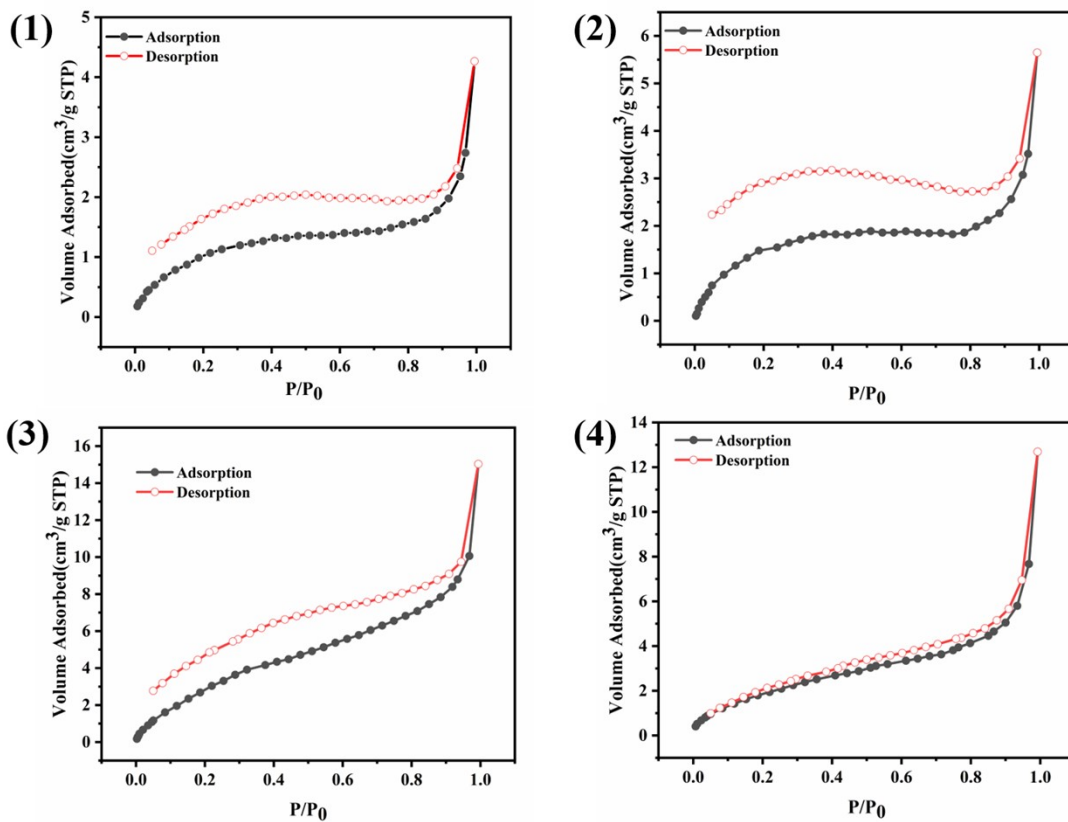


Fig. S1. The N_2 sorption isotherms for 1-4 at 77 K.

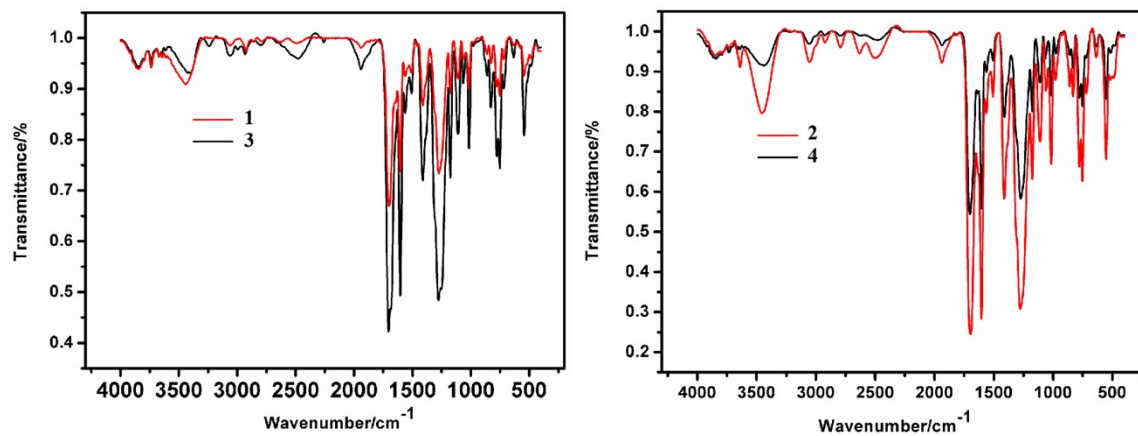


Fig. S2. IR spectra of 1-4.

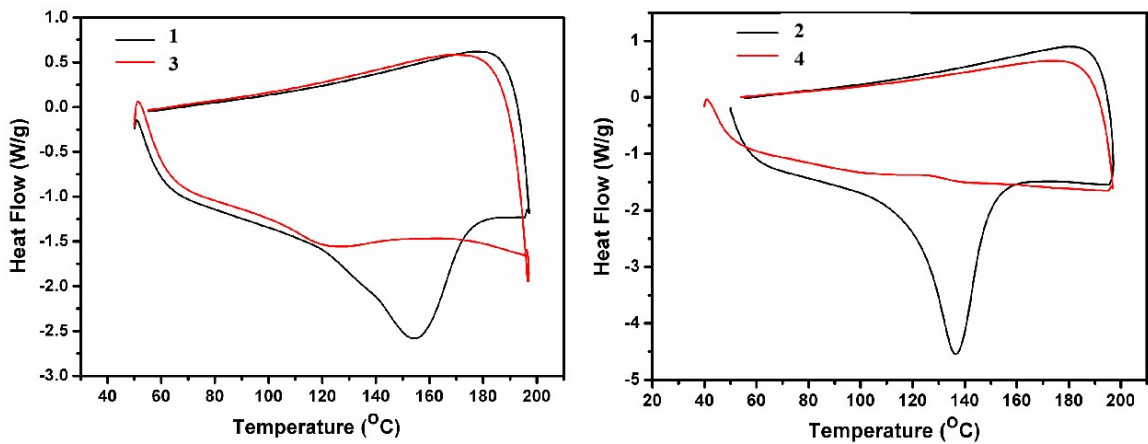


Fig. S3. DSC curves of 1–4 within 200 °C.

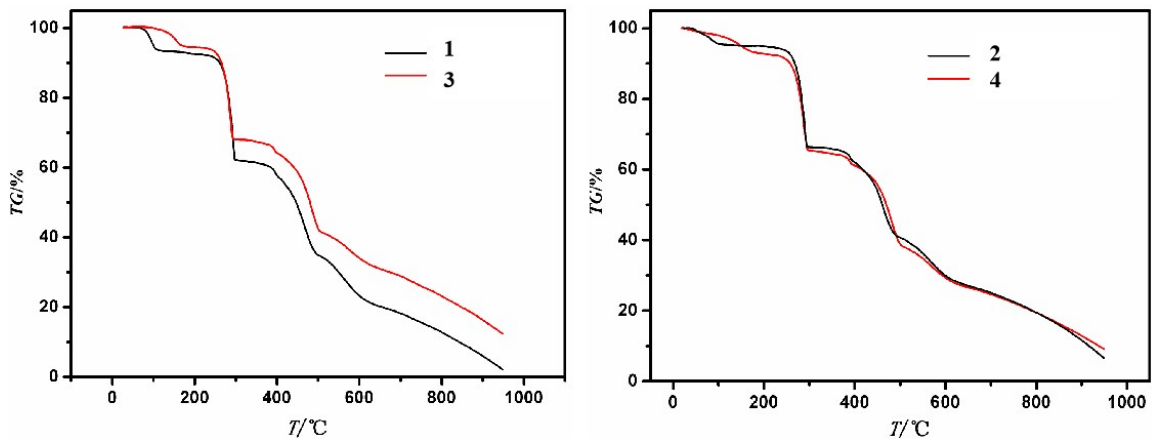


Fig. S4. TGA curves of 1–4 in the range of 25-950 °C under N₂ atmosphere.

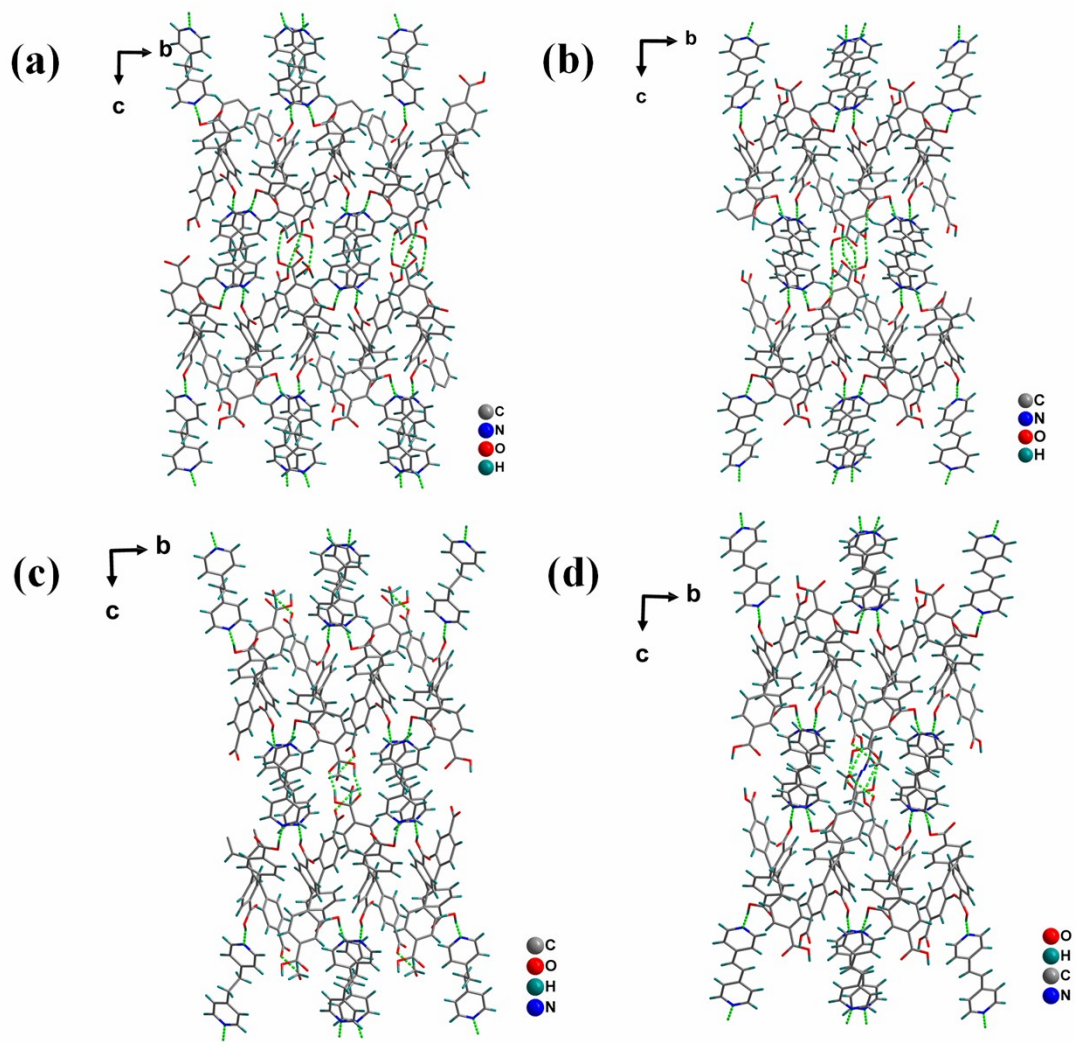


Fig. S5. 3D structure of HOFs 1–4 along the a -axis.

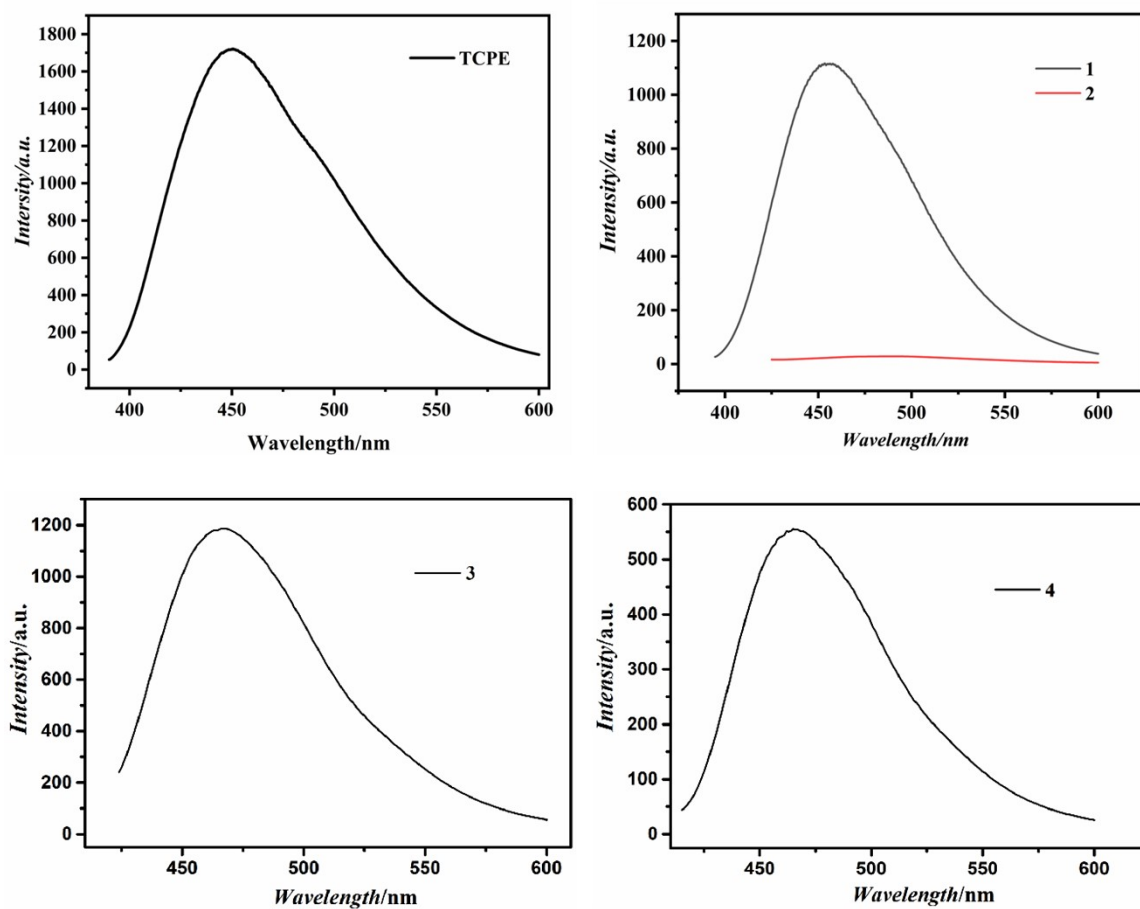
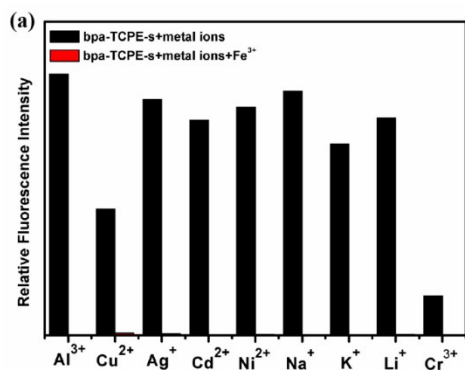


Fig. S6. Fluorescence spectra of TCPE and 1-4 at room temperature (excitation wavelength: 398 nm).



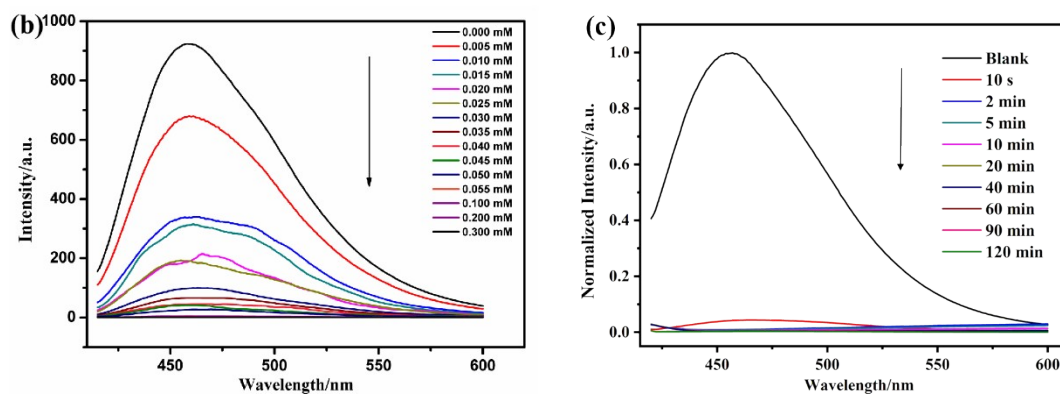


Fig. S7 (a) The influence of interfering ions on the luminescence intensity of Fe^{3+} at room temperature; (b) the influence of Fe^{3+} with different concentration at room temperature on the liquid emission spectrum of **3**; (c) Time-dependent emission spectra of the suspension after adding Fe^{3+} (0.2 M) at room temperature ($\lambda_{\text{ex}} = 396 \text{ nm}$).

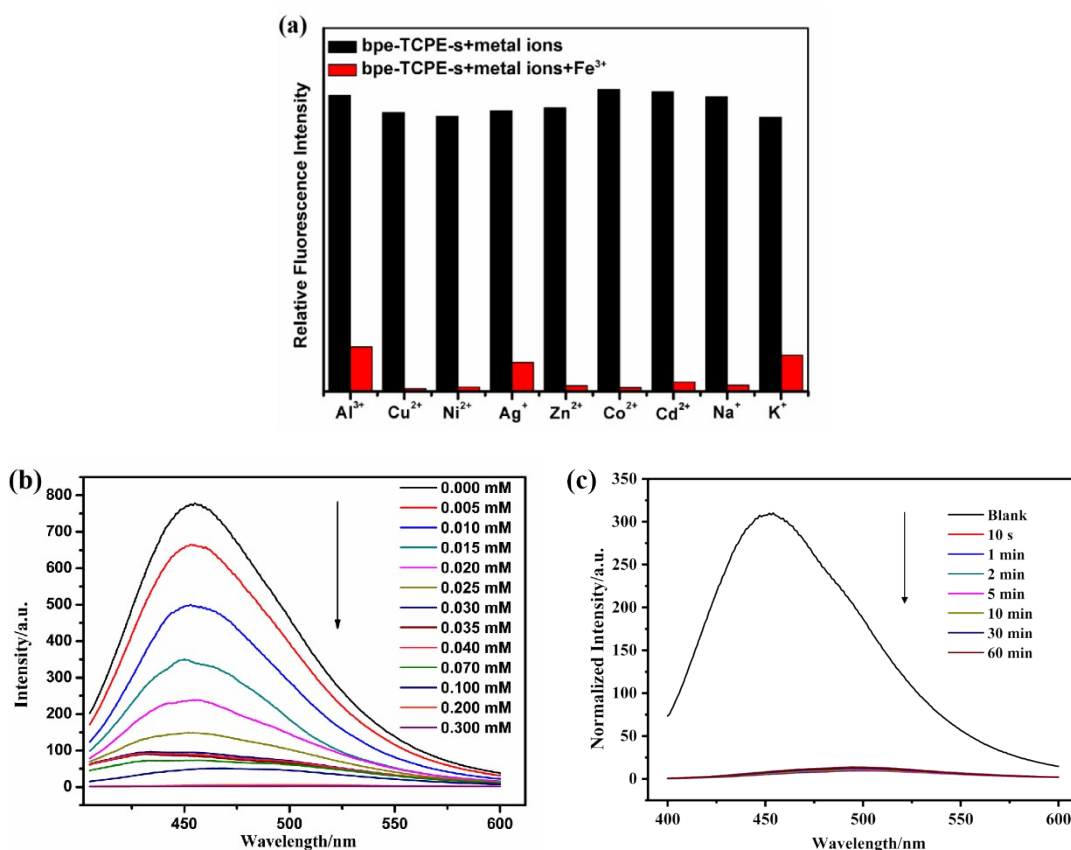


Fig. S8 (a) The influence of interfering ions on the luminescence intensity of Fe^{3+} at room temperature; (b) the influence of Fe^{3+} with different concentration at room temperature on the liquid emission spectrum of **4**; (c) Time-dependent emission spectra of the suspension after adding Fe^{3+} (0.2 M) at room temperature ($\lambda_{\text{ex}} = 376 \text{ nm}$).

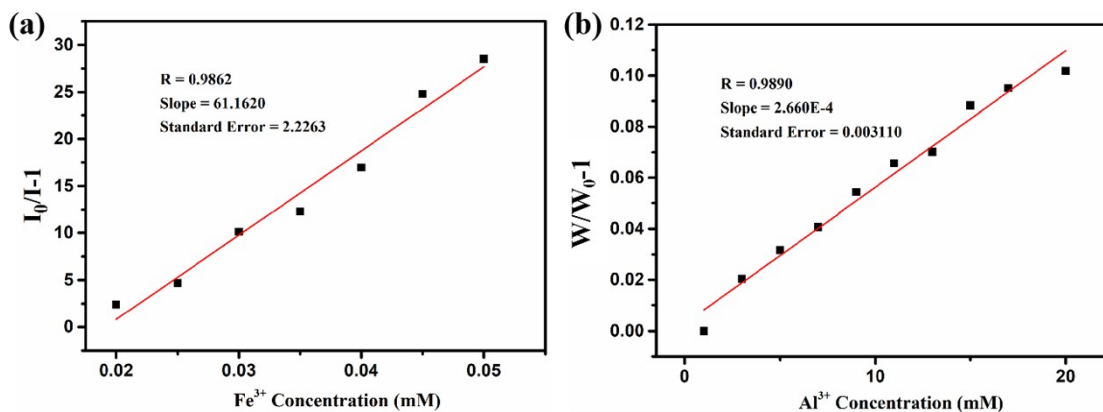


Fig. S9. Correlation between the luminescence of **3** and the concentration of Fe^{3+} (a) and Al^{3+} (b).

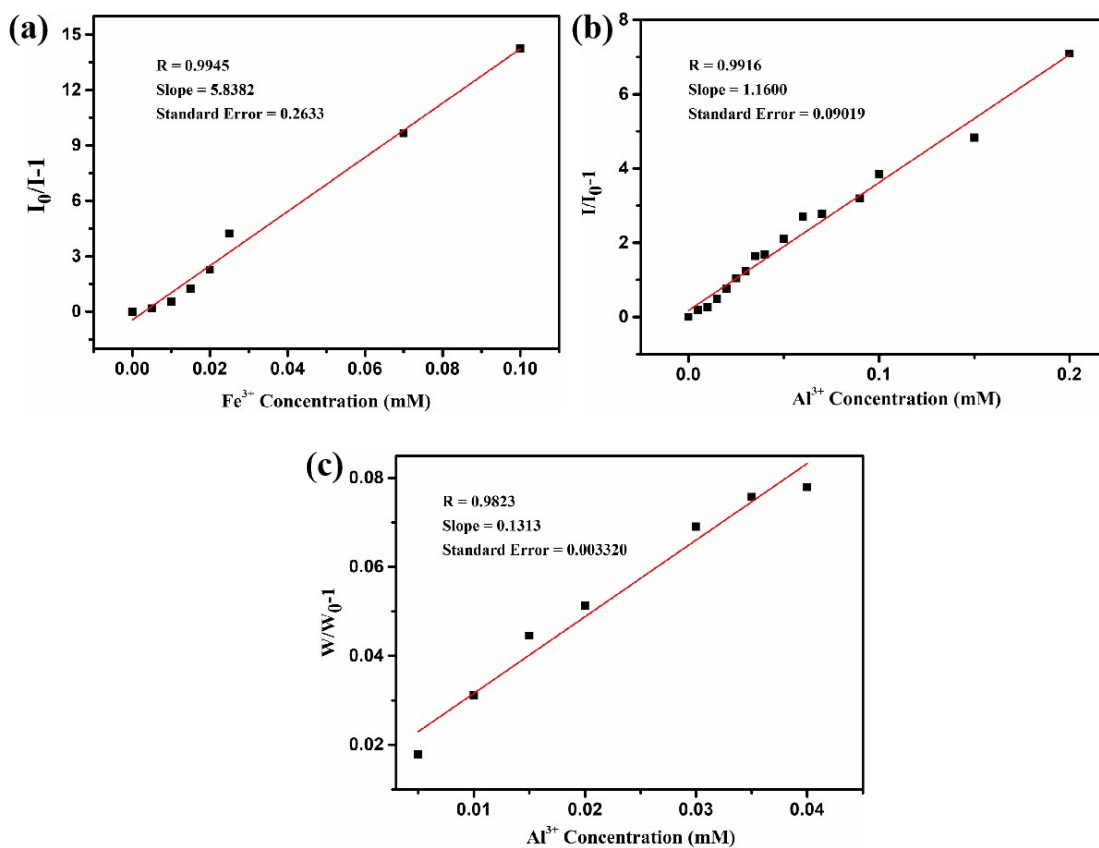


Fig. S10. (a) Correlation between the luminescence of **4** and the concentration of Fe^{3+} . (b) The photoluminescence intensities correlation between the luminescence of **4** and the concentration of Al^{3+} . (c) The fluorescence maximum peak wavelengths correlation between the luminescence of **4** and the concentration of Al^{3+} .

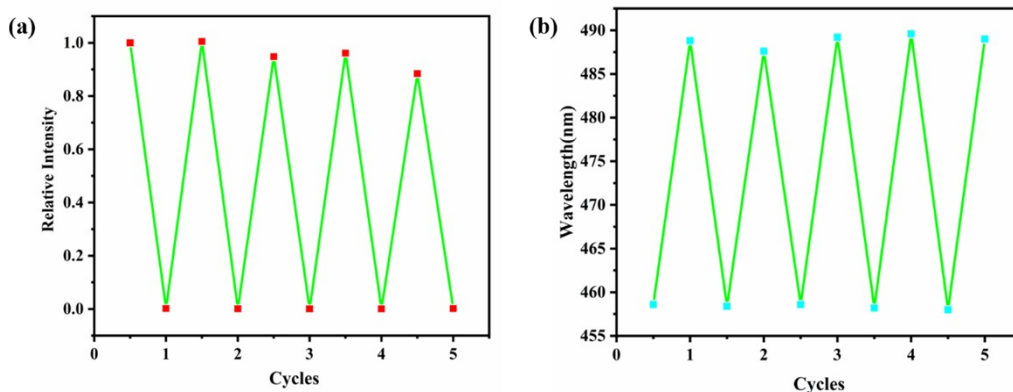


Fig. S11. Relative luminescent intensity of **3** after five runs of recycling experiments for (a) Fe^{3+} , and the red-shift emission of **3** after five runs of recycling experiments for (b) Al^{3+} .

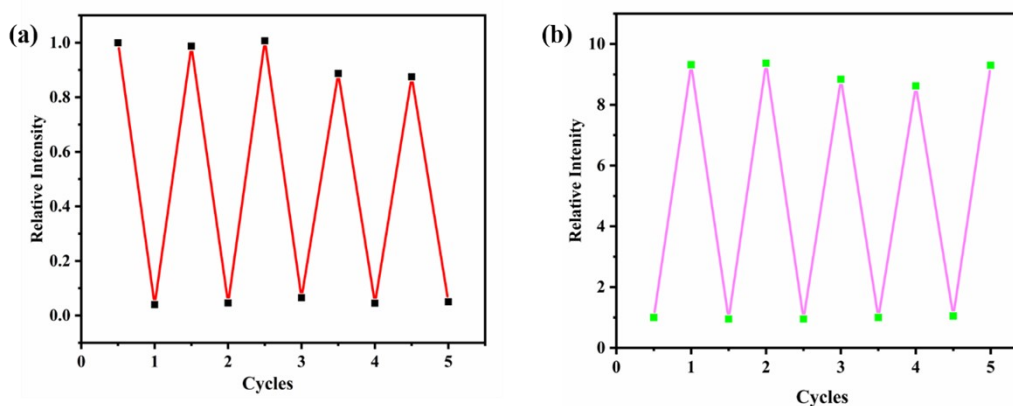


Fig. S12. Relative luminescent intensity of **4** after five runs of recycling experiments for (a) Fe^{3+} , and (b) Al^{3+} .

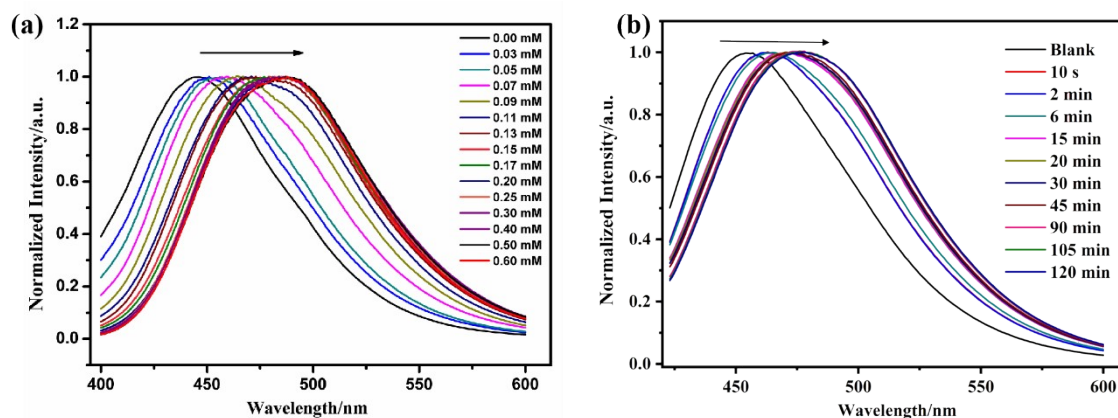


Fig. S13. (a) Liquid emission spectra of **3** upon the addition of different concentrations of Al^{3+} at room temperature; (b) Time-dependent emission spectra of the suspension after adding Al^{3+} (0.2 M) at room temperature ($\lambda_{\text{ex}} = 396 \text{ nm}$).

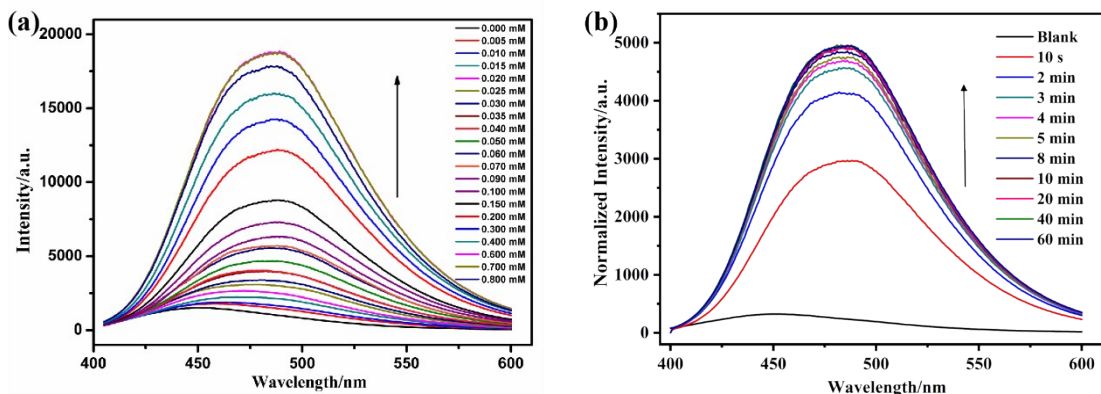


Fig. S14. (a) Liquid emission spectra of **4** upon addition of different concentrations of Al^{3+} at room temperature ($\lambda_{\text{ex}} = 376 \text{ nm}$); (b) Time-dependent emission spectra of the suspension after adding Al^{3+} (0.2 M) at room temperature ($\lambda_{\text{ex}} = 376 \text{ nm}$).

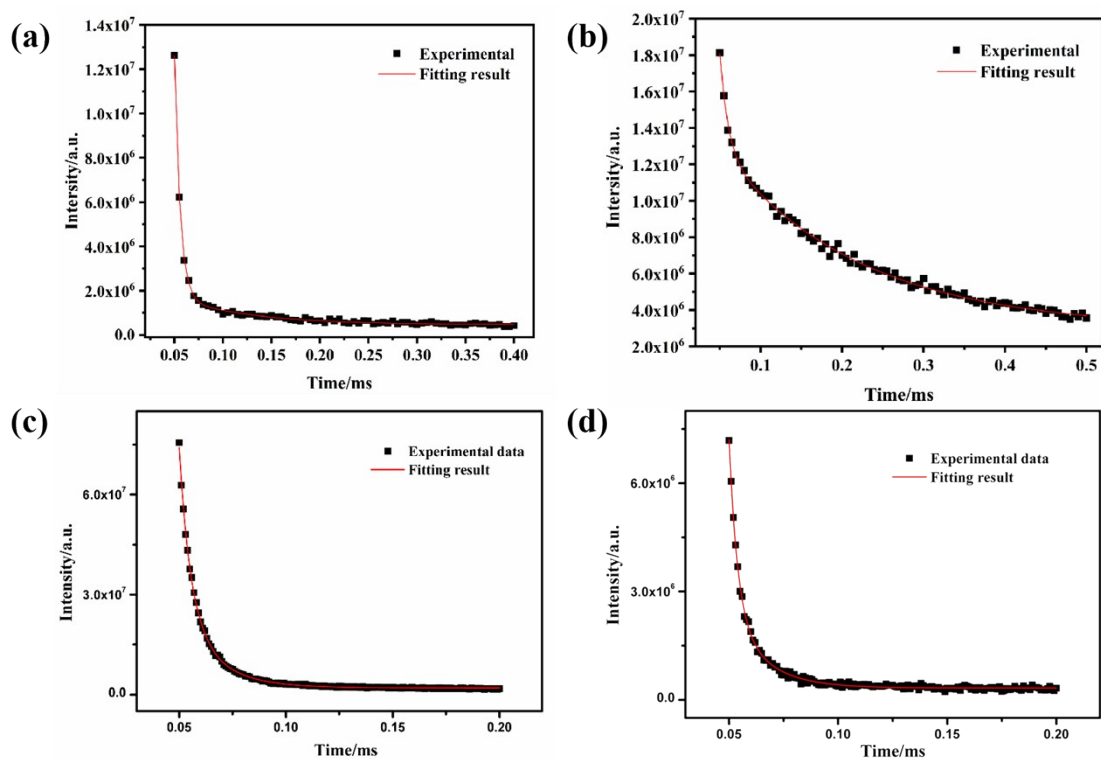


Fig. S15. The luminescence decay of HOFs **1**(a), **2**(b), **3**(c) and **4**(d), respectively ($\lambda_{\text{ex}} = 398 \text{ nm}$, $\lambda_{\text{em}} = 456 \text{ nm}$ for **1**, $\lambda_{\text{ex}} = 398 \text{ nm}$, $\lambda_{\text{em}} = 488 \text{ nm}$ for **2**, $\lambda_{\text{ex}} = 398 \text{ nm}$, $\lambda_{\text{em}} = 466 \text{ nm}$ for **3** and $\lambda_{\text{ex}} = 398 \text{ nm}$, $\lambda_{\text{em}} = 472 \text{ nm}$ for **4**).

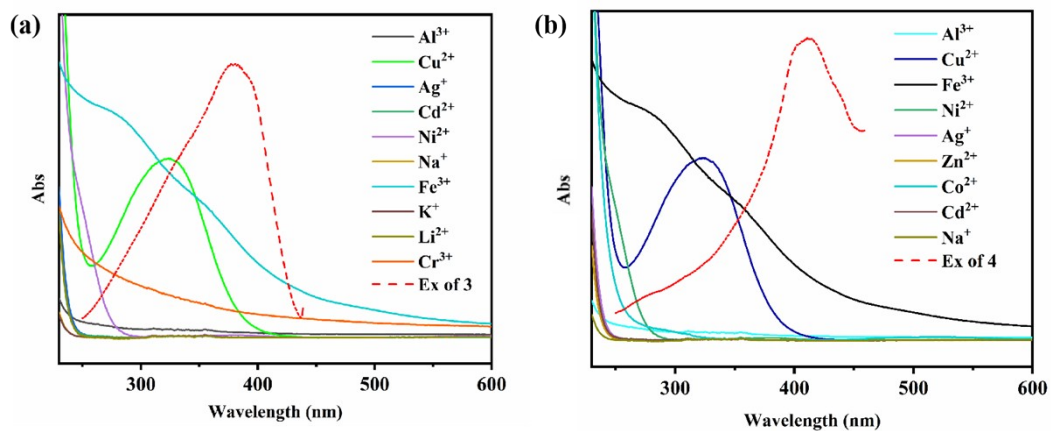


Fig. S16. UV-vis adsorption spectra of **3** upon the addition of different $\text{M}(\text{NO}_3)_x$ and the excitation spectrum of **3** (a), and UV-vis adsorption spectra of **4** upon the addition of different $\text{M}(\text{NO}_3)_x$ and the excitation spectrum of **4** (b).